Nonlinear intersubband absorption of a hot quasi-two-dimensional electron plasma studied by femtosecond infrared spectroscopy

Stephan Lutgen, Robert A. Kaindl, Michael Woerner, and Thomas Elsaesser
Max-Born-Institut für Nichtlineare Optik und Kurzzeitspektroskopie, D-12489 Berlin, Germany

Andreas Hase and Harald Künzel
Heinrich-Hertz-Institut für Nachrichtentechnik Berlin GmbH, D-10587 Berlin, Germany

(Received 26 August 1996)

The transient $(n=1)$ to $(n=2)$ intersubband absorption of a pure electron plasma in n-type $Ga_{0.48}In_{0.53}As/Al_{0.48}In_{0.52}As$ quantum wells is studied in femtosecond pump-probe experiments. The ultrafast dynamics of nonlinear absorption shows strong changes when tuning the midinfrared pulses over the intersubband absorption line. The nonlinear optical response is determined by both intersubband relaxation with a time constant of 1.3 ps and the intraband dynamics of $(n=1)$ electrons, which are monitored in an independent experiment. [S0163-1829(96)51748-0]

The quantization of electron and hole states in low-dimensional semiconductors leads to a sequence of valence and conduction subbands and a new type of elementary excitation, the optical intersubband (IS) transition between consecutive bands. The linear and nonlinear optical properties of IS excitations in quasi-two-dimensional semiconductors are important both from the viewpoint of the underlying carrier dynamics and for novel optoelectronic devices like the quantum cascade laser[1] or photodetectors[2] for the infrared range. The optical transition between the $(n=1)$ and $(n=2)$ conduction subbands in quantum wells (QW's) is dipole allowed and exhibits a very high absorption cross section of the order of 10^{-14} cm^2. Under intense resonant excitation of this transition, a strong nonlinear increase of transmission has been observed in quasistationary saturation measurements[3] and in picosecond pump-probe studies,[4,5] the latter showing a picosecond decay of enhanced transmission.

The dynamics of IS excitations are governed by scattering processes of the optically excited carriers, including IS as well as intrasubband relaxation. The dynamics of nonlinear IS absorption observed in Refs. 3 and 5 have been interpreted in terms of population relaxation from the upper to the lower subband whereas in Refs. 4 and 6 real-space transfer of carriers to potential minima in the barriers of the QW structures has been invoked to account for the picosecond decay times. Such an analysis neglects the in-plane dispersion of the subbands (energy versus in-plane k vector) and the distribution of carriers in k space. However, band-structure calculations[7] and experimental studies of IS absorption profiles[8] indicate different effective masses and nonparabolicities of the two subbands which lead to a k-dependent energy of the IS transition as depicted schematically in Fig. 1(a). Furthermore, recent experiments on electrons in $GaAs/Al_{1-y}Ga_yAs$ and $Ga_{1-x}In_xAs/Al_{1-y}In_yAs$ quantum wells give similar time scales of IS relaxation occurring with time constants of 0.5 to 1 ps (Refs. 9–12) and intraband thermalization of backscattered $(n=1)$ carriers within 2 ps.[10] Thus, transient changes of the carrier distribution by intraband scattering processes should contribute to the dynamics of nonlinear IS absorption on a picosecond time scale, a phenomenon that has not been explored until now.

In this paper, we report a femtosecond study of nonlinear intersubband absorption in $Ga_{0.48}In_{0.53}As/Al_{0.48}In_{0.52}As$ quantum wells. One-color measurements with femtosecond pump and probe pulses in the midinfrared demonstrate that the dynamics and the sign of nonlinear IS absorption change

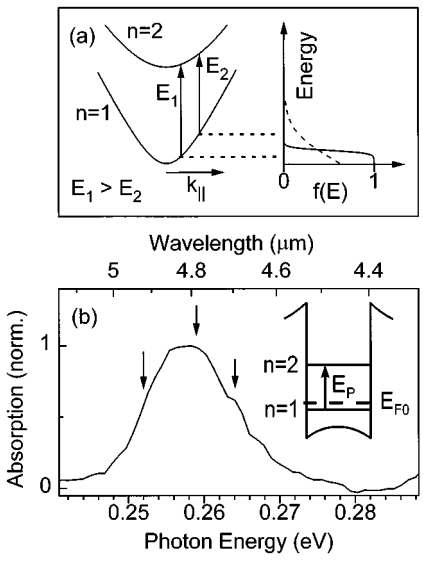

FIG. 1. (a) Schematic of the in-plane dispersion of the $(n=1)$ and $(n=2)$ conduction subbands. Right hand side: cold (solid line) and hot (dashed line) electron distributions. (b) Steady state intersubband absorption between the $(n=1)$ and $(n=2)$ conduction subband of the n-type modulation-doped $Ga_{0.48}In_{0.53}As/Al_{0.48}In_{0.52}As$ multiple-quantum-well (MQW) structure (well width 6 nm, electron concentration 1.5×10^{11} cm^{-2}). The spectrum was measured with the sample under the Brewster angle in the infrared beam. The arrows mark the spectral position of the midinfrared pulses used in the femtosecond experiments. Insert: Schematic of the intersubband transition (E_{F0}: initial Fermi level of the electrons).

strongly with the spectral position within the IS absorption line. Complementary experiments probing $(n=1)$ valence- to conduction-band transitions provide independent insight into the transient electron distributions occurring after IS excitation. We demonstrate, to our knowledge for the first time, that the dynamics of nonlinear IS absorption in the midinfrared is strongly influenced by the intraband redistribution of $(n=1)$ electrons.

In our experiments, we studied an n-type modulation-doped multiple-quantum-well structure which was grown by molecular-beam epitaxy on an InP substrate. The sample consists of 50 $Ga_{0.47}In_{0.53}As$ QW's of 6 nm width separated by 14-nm-thick $Al_{0.48}In_{0.52}As$ barriers. The structures are Si δ doped in the center of the barriers, resulting in an electron density of 1.5×10^{11} cm^{-2} in each quantum well. The steady-state IS absorption spectrum of this sample is plotted in Fig. 1(b) and is centered around 258 meV (wavelength 4.8 μm). Two different femtosecond pump-probe experiments were performed at a lattice temperature of $T_L=8$ K: (i) Part of the $(n=1)$ electrons present by doping were excited to the $(n=2)$ conduction subband by a femtosecond midinfrared pulse overlapping with the IS absorption line. The resulting change of IS absorption was monitored by a weak delayed probe pulse of the same photon energy. Data were recorded for different spectral positions E_p of the midinfrared pulses, as indicated by the arrows in Fig. 1(b). To enhance the interaction of the midinfrared pulses with the IS dipole moment oriented perpendicular to the QW layers, a prism geometry of the sample was used.[4] (ii) Femtosecond IS excitation was also applied in the second experiment. Here, however, near-infrared probe pulses monitor changes of the interband absorption from the $(n=1)$ valence subbands to the $(n=1)$ conduction subband to determine transient distributions of $(n=1)$ electrons. In such measurements, the sample was put under Brewster angle in the pump beam of in-plane polarization. Pump and probe pulses were derived from a regeneratively amplified Ti:sapphire laser. Parametric frequency mixing provides midinfrared pulses of 130 fs duration (bandwidth 14 meV).[13] The 100-fs probe pulses in the near-infrared (spectral width 13 meV) were generated by spectral selection from a femtosecond white-light continuum. Excitation densities of about 15% of the total electron concentration were used in both experiments, as estimated from the respective sample transmission and spot size on the samples.

In Fig. 2(a), we present results of the one-color experiment with midinfrared pump and probe pulses. The normalized change of IS transmission $\Delta T/T_0=(T-T_0)/T_0$ is plotted as a function of delay time between pump and probe for three different spectral positions E_p (circles; T_0,T: sample transmission before and after excitation). At $E_p=259$ meV, an absolute value of $\Delta T/T_0\approx0.1$ is found. The solid lines are results of model calculations to be discussed below. At early delay times, we observe an increase of transmission that rises within the time resolution of the experiment and shows a fast partial decay during the first 2–3 ps. The signal at later delay times depends strongly on the specific spectral position. At the center of the IS absorption line ($E_p=259$ meV), it returns to zero within 6 ps. In contrast, a long-lived bleaching is observed for $E_p=264$ meV on the high-energy wing of IS absorption, whereas an induced absorption is found at $E_p=252$ meV. These slow signals decay on a time scale of 50 ps.

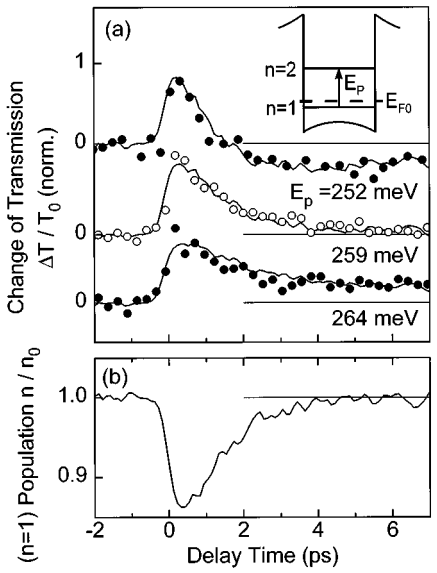

FIG. 2. (a) Time-resolved changes of intersubband absorption for different photon energies of the pump and probe pulses. The change of transmission $\Delta T/T_0=(T-T_0)/T_0$ (circles) is plotted vs the delay time between the midinfrared pump and probe pulses at the same spectral position (T,T_0: transmission with and without excitation). Solid lines: model calculations as explained in the text. Insert: pump-probe scheme. (b) Time-resolved population change in the $(n=1)$ subband as calculated from transient interband absorption spectra. The $(n=1)$ population shows a depletion that rises within the time resolution of the experiment and recovers with a time constant of 1.3 ps, the intersubband scattering time.

The second experiment provides independent information on the dynamics of $(n=1)$ electrons. Transient interband absorption spectra were measured in the range of the $(n=1)$ absorption edge around 0.955 eV. It is determined by the band gap of the QW's and by the steady-state electron distribution that populates the bottom of the $(n=1)$ conduction subband up to the initial Fermi level F_{F0} and blocks the corresponding interband transitions. In Fig. 3, the change of transmission at different delay times is plotted versus the photon energy of the probe pulses. The mid-infrared excitation pulse was centered at $E_p=260$ meV, resonant to the IS absorption line [Fig. 1(b)]. At 0.2 ps [Fig. 3(a)], a decrease of transmission occurs below the initial Fermi level E_{F0} that is due to depopulation by the midinfrared excitation pulse. At later times, this signal increases and an enhanced transmission is found above E_{F0} [Figs. 3(c)–3(e)].[14] This bleaching which is absent at early delay times gives evidence of an excess population of those higher lying $(n=1)$ states by energetic electrons. Eventually, the transmission changes decay by electron cooling within 50 ps.

In our experiments, IS excitation and subsequent relaxation lead to electron redistribution at constant density which gives rise to changes of both IS absorption in the midinfrared and of $(n=1)$ interband absorption in the near infrared. We first discuss the interband absorption spectra (Fig. 3), providing insight into the momentary distribution of $(n=1)$ electrons. Then, this information is used to analyze the nonlinear IS absorption (Fig. 2).

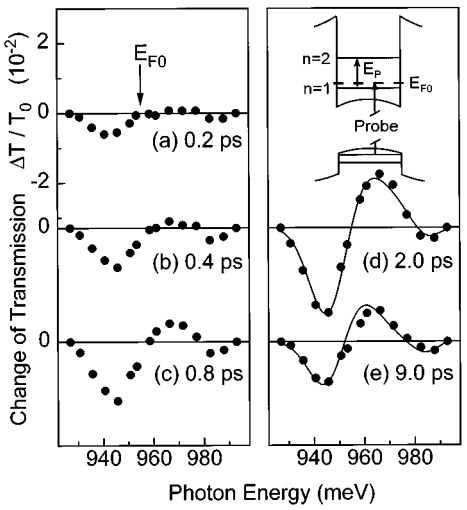

FIG. 3. Transient spectra of the n-type modulation-doped $Ga_{0.48}In_{0.53}As/Al_{0.48}In_{0.52}As$ MQW structure in the spectral range of the $(n=1)$ interband transition after femtosecond intersubband excitation. The transmission change $\Delta T/T_0$ is plotted as a function of the photon energy of the probe pulses for delay times of (a) 0.2 ps, (b) 0.4 ps, (c) 0.8 ps, (d) 2.0 ps, and (e) 9.0 ps (circles). The bandwidth of the probe pulses is 13 meV (full width at half maximum). Solid lines: calculated spectra for hot Fermi distributions with temperatures of (d) 180 K and (e) 70 K. Insert: pump-probe scheme of the experiments.

After the decay of coherent optical polarizations in the sample on a 100-fs time scale,[15] the change of interband absorption is determined by the difference between the transient and the initial distribution functions of $(n=1)$ electrons. A detailed experimental and theoretical analysis of transient $(n=1)$ interband spectra gives the following relaxation scenario of $(n=1)$ electrons:[10] IS excitation induces a depletion of $(n=1)$ states over the entire range from the $(n=1)$ band gap up to the initial Fermi level E_{F0}, which is evident from the reduced transmission in the spectra at early delay times [Fig. 3(a)]. The subsequent formation of a high-energy tail in the carrier distribution leads to an enhancement of this transmission decrease and a delayed transmission increase at energies above E_{F0} at delay times between 0.4 and 2 ps. IS relaxation of $(n=2)$ electrons back to high-lying $(n=1)$ states and subsequent intraband redistribution of energetic and formerly cold carriers by inelastic Coulomb scattering represent the main mechanisms forming the high-energy tail in this athermal distribution. After about 2 ps, a hot quasiequilibrium distribution of $(n=1)$ electrons is reached, connected with similar amplitudes of the transmission decrease below and the bleaching above E_{F0}. The spectra in Fig. 3(d) and 3(e) are well reproduced by a Fermi distribution with a carrier temperature of 180 K and 70 K, respectively (solid lines). At even later times, the transmission changes decay by carrier cooling within 50 ps.

Quantitative information on the momentary overall population of the $(n=1)$ subband is obtained by spectrally integrating the transient distribution function underlying the spectra of Fig. 3. The result plotted in Fig. 2(b) shows a depletion of the $(n=1)$ subband by up to 15% due to femtosecond IS excitation. At later times, IS relaxation back to $(n=1)$ subband leads to a recovery of population with a time constant of about 1.3 ps, in good agreement with directly measured IS scattering times.[9,10]

Next, we discuss the transient changes of IS absorption presented in Fig. 2(a). Those are determined by the difference of the time-dependent electron distributions in the $(n=1)$ and $(n=2)$ conduction subbands. Different parts of the distributions dominate the signal at different spectral positions E_p within the IS absorption line, as can be visualized with the help of the schematic subband dispersion in Fig. 1(a). The two subbands have different effective in-plane masses and nonparabolicities. At photon energies on the high-energy wing of the IS absorption line [arrow E_1 in Fig. 1(a)], one preferentially excites and probes states close to the minima of the two subbands. In contrast, IS absorption at small photon energies (arrow E_2) is connected with optical coupling of higher-lying states at larger $k_\parallel$ values.

The depletion of $(n=1)$ states and the population of $(n=2)$ states by IS excitation lead to an increase of IS transmission. At all spectral positions, the magnitude of this bleaching is proportional to the density of absorbed infrared photons and occurs within the time resolution of the experiment. The subsequent time evolution depends strongly on the spectral position. At the center of the IS absorption line $(E_p=259$ meV), the bleaching follows a decay kinetics similar to the recovery of the overall $(n=1)$ population plotted in Fig. 2(b). Here, the probe pulses average over depleted $(n=1)$ states below and transiently populated states above the initial Fermi level E_{F0}, the contributions of which are of opposite sign and roughly cancel each other in the overall transmission change. Consequently, the time-resolved bleaching is mainly determined by IS scattering from the $(n=2)$ to the $(n=1)$ subband. In contrast, the data recorded in the wings of the IS absorption line ($E_p=252$ and 264 meV) exhibit a different decay kinetics at early times and transmission changes that persist much longer than the recovery of the $(n=1)$ population. *Here, the dynamics of nonlinear IS absorption reflects both IS scattering and intraband redistribution within the* $(n=1)$ *subband*. At $E_p=264$ meV, the long-lived depletion of population at the bottom of the $(n=1)$ subband which is evident from the data in Fig. 3, leads to a slowing down in the decay of the bleaching signal. The much faster decay of the bleaching and the subsequent enhanced absorption at $E_p=252$ meV are caused by the transient excess populations on the high-energy tail of the $(n=1)$ distributions. Both the high-energy tail and the depletion at the bottom of the $(n=1)$ subband decay by carrier cooling on a slow time scale of several tens of picoseconds.

Our qualitative interpretation of the nonlinear IS absorption is supported by model calculations. The in-plane dispersion of the $(n=1)$ and $(n=2)$ subband was approximated with an effective electron mass of $0.05m_0$ and $0.065m_0$, respectively (m_0: free electron mass).[7] A k-independent IS dipole moment was used. The transient IS absorption at a given transition energy was calculated from the difference between the $(n=1)$ and $(n=2)$ distribution taken at the specific electron energy. The $(n=1)$ electron distribution was derived from the interband spectra in Fig. 3. Over the optically coupled range, the $(n=2)$ distribution is assumed to be k independent and to decay with the IS relaxation time of 1.3 ps. The solid lines in Fig. 2(a) represent the calculated absorption change after convolution with the spectral profiles

of the infrared pulses. The good agreement with the data emphasizes the contribution of the $(n=1)$ intrasubband relaxation to the nonlinear IS absorption dynamics.

In summary, the dynamics of nonlinear intersubband absorption of electrons in $Ga_{0.48}In_{0.53}As/Al_{0.48}In_{0.52}As$ quantum wells depend strongly on the spectral position within the intersubband absorption line. The sign and the dynamics of the transmission changes are determined by both intersubband scattering from the $(n=2)$ back to the $(n=1)$ subband with a time constant of about 1.3 ps as well as by electron redistribution processes within the lower subband. The transient depletion of states at the bottom of the $(n=1)$ subband and the formation of a high-energy tail in the electron distribution lead to a bleaching on the high-energy wing and an enhanced absorption on the low-energy wing of the IS absorption line, respectively. These absorption changes persist even after the complete depopulation of the upper subband and decay by electron cooling within 50 ps.

We gratefully acknowledge support from the Deutsche Forschungsgemeinschaft (SFB 296) and from the European Commission through the ULTRAFAST network.

[1] J. Faist, F. Capasso, L. Sivco, C. Sirtori, A. L. Hutchinson, and A. Cho, Science **264**, 553 (1994).

[2] B. F. Levine, K. K. Choi, C. G. Bethea, J. Walker, and R. J. Malik, Appl. Phys. Lett. **50**, 1092 (1987).

[3] F. H. Julien, J. M. Lourtioz, N. Herschkorn, D. Delacourt, J. P. Pocholle, M. Papuchon, R. Planel, and G. Le Roux, Appl. Phys. Lett. **53**, 116 (1988).

[4] A. Seilmeier, H. J. Hübner, G. Abstreiter, G. Weimann, and W. Schlapp, Phys. Rev. Lett. **59**, 1345 (1987).

[5] J. N. Heyman *et al.*, Appl. Phys. Lett. **68**, 3019 (1996).

[6] S. M. Goodnick and J. E. Lary, Semicond. Sci. Technol. **7**, B109 (1992).

[7] U. Ekenberg, Phys. Rev. B **36**, 6152 (1987).

[8] R. J. Baeuerle, T. Elsaesser, H. Lobentanzer, W. Stolz, and K. Ploog, Phys. Rev. B **40**, 10 002 (1989).

[9] M. C. Tatham, J. F. Ryan, and C. T. Foxon, Phys. Rev. Lett. **63**, 1637 (1989).

[10] S. Lutgen, R. A. Kaindl, M. Woerner, T. Elsaesser, A. Hase, H. Künzel, M. Gulia, D. Meglio, and P. Lugli, Phys. Rev. Lett. **77**, 3657 (1996).

[11] J. Faist *et al.*, Appl. Phys. Lett. **63**, 1354 (1993).

[12] A. P. Heberle, W. W. Ruehle, and K. Koehler, Phys. Status Solidi B **173**, 381 (1992).

[13] F. Seifert, V. Petrov, and M. Woerner, Opt. Lett. **19**, 2009 (1994).

[14] For probe energies between 935 and 975 meV the signal is exclusively determined by the $(n=1)$ heavy-hole to conduction-band transition. Above 975 meV, the $(n=1)$ light-hole to conduction-band transition makes a small contribution, probing electron states below E_{F0}. No transmission change was detected above 990 meV.

[15] Very recently, this time scale of IS phase relaxation was observed in midinfrared four-wave-mixing measurements, which will be discussed elsewhere.